

VERITAS Observations of the Vicinity of the Cygnus Cocoon

A. Weinstein for the VERITAS Collaboration
Iowa State University, 1 Osborne Dr., Ames, IA, 50011, USA

The study of γ -ray emission from galactic sources such as supernova remnants (SNR) may provide key insights into their potential role as accelerators of cosmic rays up to the knee ($\sim 10^{15}$ eV). The VERITAS Observatory is sensitive to galactic and extragalactic γ -ray sources in the 100 GeV to 30 TeV energy range. We report here on VERITAS observations of the vicinity of the cocoon of freshly accelerated cosmic rays reported by Fermi, which lies between potential accelerators in the Cygnus OB2 association and the γ -Cygni SNR. A particular focus is placed on the source VER J2019 +407 in γ -Cygni.

1. The VERITAS Instrument

VERITAS, located at the Fred Lawrence Whipple Observatory near Tucson, Arizona, is an array of four 12-meter imaging atmospheric Cherenkov telescopes. Each telescope has a pixelated camera comprised of 499 photomultiplier tubes with a 3.5° field of view. Designed to detect photons of astrophysical origin between 100 GeV and 30 TeV, VERITAS detects and images the secondary Cherenkov light produced when gamma rays and cosmic rays initiate particle cascades in the upper atmosphere. Stereoscopic reconstruction of events using multiple telescopes allows for single-photon angular resolution of better than 0.1° and energy resolution on the order of 15-25%. In its current configuration, VERITAS can detect a source with $\sim 1\%$ of the Crab Nebula flux in less than 30 hours. The instrument has been operating in full array mode since 2007. See [Holder et al. 2006] for further details regarding the operation of VERITAS.

2. The γ -Cygni Supernova Remnant

SNR G78.2+2.1, also known as the γ -Cygni supernova remnant (SNR), is a $\sim 1^\circ$ diameter shell-like radio and X-ray SNR [Higgs et al. 1977, Lozinskaya et al. 2000]. It is estimated to be at a distance of ~ 1.7 kpc [Higgs et al. 1977, Lozinskaya et al. 2000] and to be approximately 5000 – 7000 years old [Higgs et al. 1977, Landecker et al. 1980]. It is thought to be in an early phase of adiabatic expansion into a low-density medium [Lozinskaya et al. 2000]. A slowly expanding H I shell immediately surrounding the radio shell was found by Gosachinskij [2001], which Lozinskaya et al. [2000] believes to have been created by the progenitor stellar wind.

The radio shell divides roughly into northern and southern arcs [Uchiyama et al. 2002, Zhang et al. 1997]. Enhanced thermal X-ray emission in the north suggests shocked gas [Uchiyama et al. 2002] and falls in a void of CO emission [Ladouceur & Pineault 2008]. Strong optical emission with sulfur lines also characterizes the region [Mavromatakis 2003]. The γ -ray

satellite *Fermi*, operating at GeV energies, has discovered a γ -ray pulsar PSR J2021+4026 at the center of the remnant [Abdo et al. 2010a,b]. While this pulsar has a low luminosity (1.1×10^{35} erg s⁻¹) and a spin-down age (76.8 kyr) much greater than the estimated age of SNR G78.2+2.1, the pulsar kinematics make it probable that PSR J2021+4026 was born with something close to its current spin period and is the remnant of SNR G78.2+2.1's progenitor star [Trepl et al. 2010]. Diffuse γ -ray emission above 10 GeV is also reported by *Fermi* over the full extent of the remnant [Lande et al. 2012]. A point source co-located with VER J2019+407 was previously reported in the first and second *Fermi* catalogs [Abdo et al. 2010a, Nolan et al. 2012], but Lande et al. [2012] conclude it to be artifact.

3. The Cygnus Cocoon

Ackermann et al. [2011] reported an extended region of emission above a few GeV that they interpreted as a freshly accelerated cocoon of cosmic rays. The cavity defining the cocoon region is outlined by ionization fronts visible in the mid- infrared. γ -Cygni overlaps one end of the cocoon and is a potential source of the cocoon's trapped cosmic rays.

4. Detection of γ -ray Emission from the Direction of γ -Cygni

Figure 1 displays the acceptance-corrected very-high-energy (VHE) γ -ray excess map of the area around SNR G78.2+2.1 [Aliu et al. 2013]. An extended source is seen overlapping the northern edge of the remnant, with a detection significance of 7.5 standard deviations. We use a binned, extended maximum-likelihood fit to the raw counts map to assess the VER J2019+407 morphology. The source is modeled in the fit as a symmetric, two-dimensional Gaussian convolved with the VER J2019+407 point-spread function (PSF); the background is assumed to be flat before exposure effects are taken into

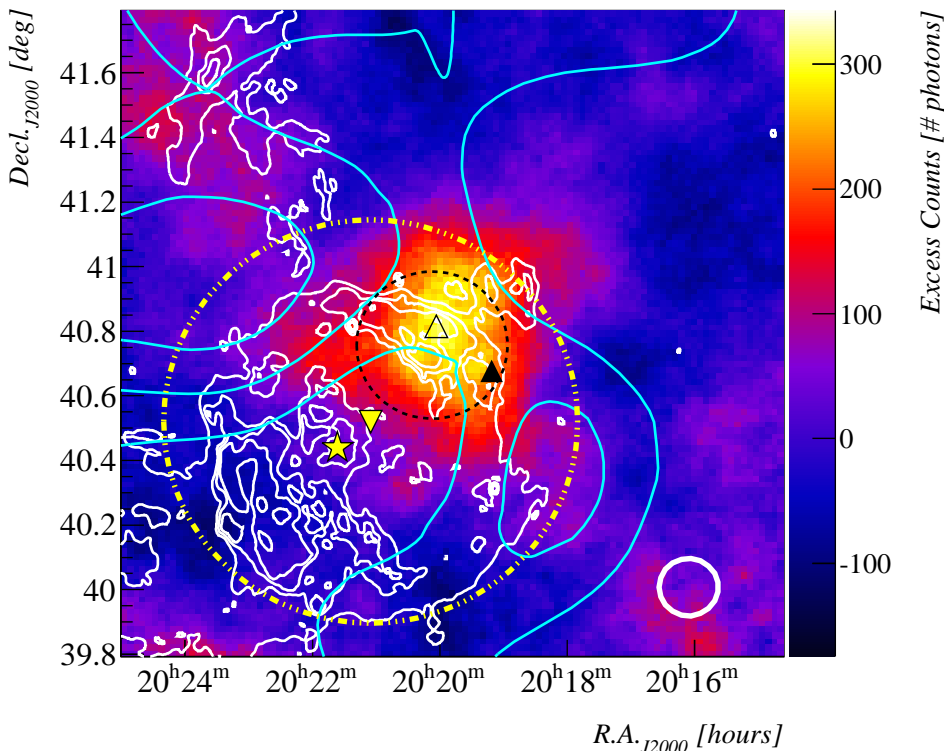


Figure 1: VERITAS γ -ray image of SNR G78.2+2.1 showing the detection of VER J2019+407 and its fitted extent (black dashed circle). CGPS 1420 MHz continuum radio contours at brightness temperatures of 23.6K, 33.0K, 39.6K, 50K and 100K (white) [Taylor et al. 2003] outline the radio SNR; the star symbol shows the location of the central γ -ray pulsar PSR J2021+4026. The inverted triangle and dot-dashed circle (yellow) show the fitted centroid and extent of the emission detected by *Fermi* above 10 GeV. The open and filled triangles (black) show the positions of *Fermi* catalog sources 1FGL J2020.0+4049 and 2FGL J2019.1+4040. The 0.16, 0.24, and 0.32 photons/bin contours of the *Fermi* detection of the Cygnus cocoon are shown in cyan. The white circle (bottom right corner) indicates the 68% containment size of the VERITAS γ -ray PSF for this analysis.

account. We find a fitted extension of the two-dimensional Gaussian to be $0.23^\circ \pm 0.03_{\text{stat}}^{+0.04^\circ}_{-0.02^\circ_{\text{sys}}}$, with fitted centroid coordinates R.A. $20^{\text{h}}20^{\text{m}}04.8^{\text{s}}$, Decl. $+40^\circ45'36''$ (J2000). The statistical uncertainty in the centroid location is 0.03° , with a systematic uncertainty of 0.018° . The systematic uncertainty considers both the telescope pointing error and systematic errors of the fit itself [Aliu et al. 2013]. The positions of the γ -ray pulsar PSR J2021+4026 (1FGL J2021.5+4026) ($\sim 0.5^\circ$ from VER J2019+407) and the centroid of the emission above 10 GeV from the remnant (as seen by *Fermi*) are also shown for reference.

Figure 2 shows the spectrum of reconstructed γ -ray events within 0.24° from R.A. $20^{\text{h}}19^{\text{m}}48^{\text{s}}$, Decl. $+40^\circ54'00''$. Runs where only three of four telescopes were operational have been excluded from this sample [Aliu et al. 2013]. The photon spectrum is consistent with a differential power law in energy,

$dN/dE = N_0 \times (E/\text{TeV})^{-\Gamma}$, between the analysis threshold of 320 GeV and 10 TeV. The photon index is $\Gamma = 2.37 \pm 0.14_{\text{stat}} \pm 0.20_{\text{sys}}$ and the flux normalization at 1 TeV is $N_0 = (1.5 \pm 0.2_{\text{stat}} \pm 0.4_{\text{sys}}) \times 10^{-12} \text{ ph TeV}^{-1} \text{ cm}^{-2} \text{ s}^{-1}$. The integral flux above 320 GeV ($5.2 \pm 0.8_{\text{stat}} \pm 1.4_{\text{sys}} \times 10^{-12} \text{ ph cm}^{-2} \text{ s}^{-1}$) corresponds to 3.7% of the Crab Nebula flux above that energy [Aliu et al. 2013].

4.1. γ -Cygni in X-Rays

Figure 3 illustrates the region of enhanced X-ray emission overlapping VER J2019+407 [Aliu et al. 2013]. It displays the 0.7 – 3.0 keV exposure-corrected X-ray map using data from ASCA Sequence #25010000 (data originally presented by Uchiyama et al. [2002]), generated by co-adding data from the two gas imaging spectrometers. A spectrum was extracted from a $12' \times 24'$ elliptical region enclos-

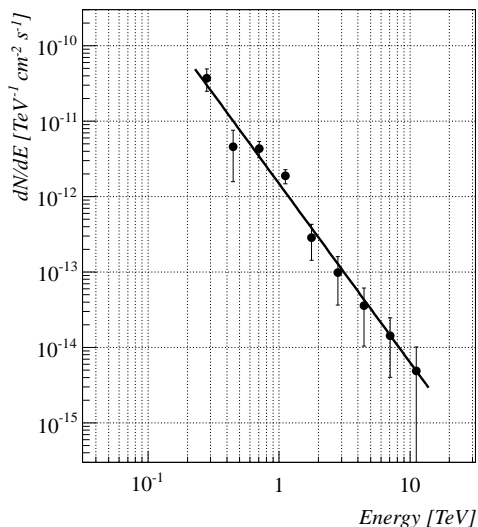


Figure 2: Spectrum of VER J2019+407, derived from 4-telescope data only. Points are the VERITAS spectrum; the line is a power-law fit with a spectral index of $\Gamma = 2.37 \pm 0.14_{\text{stat}} \pm 0.20_{\text{sys}}$ and a flux normalization of $N_0 = (1.5 \pm 0.2_{\text{stat}} \pm 0.4_{\text{sys}}) \times 10^{-12} \text{ ph TeV}^{-1} \text{ cm}^{-2} \text{ s}^{-1}$.

ing most of the X-ray emission inside the VERITAS contours, centered on coordinates R.A. $20^{\text{h}} 20^{\text{m}} 17^{\text{s}}$, Decl. $+40^{\circ} 45' 41''$ (J2000) and oriented with position angle 60° . We selected background photons from an identically sized ellipse near the center of the remnant at R.A. $20^{\text{h}} 19^{\text{m}} 38^{\text{s}}$, Decl. $+40^{\circ} 27' 02''$ (J2000), with position angle is 130° . The source and background regions are displayed in Figure 3.

The source spectrum between 0.7 and 3.0 keV is shown in Figure 4 [Aliu et al. 2013]. The X-ray spectrum was modeled using an absorbed Raymond-Smith thermal plasma model with a best-fit temperature of $kT = 0.57 \pm 0.14$ keV. With this model the column density is $N_H = (3.7 \pm 2.0) \times 10^{21} \text{ cm}^{-2}$, the normalization is $N = 1.8 \times 10^{-3} \text{ cm}^{-5} \text{ m}$ and the absorption-corrected flux is $6.0 \times 10^{-12} \text{ erg cm}^{-2} \text{ s}^{-1}$ in the 0.5–8.0 keV band. This result differs significantly from that given in [Uchiyama et al. 2002], which claimed an additional power-law component and a large Ne IX line feature. The divergence in results appears to hinge, not on the choice of source region, which is similar, but on the choice of background region [Aliu et al. 2013]. We selected a background region that was as close as possible to the source while [Uchiyama et al. 2002] chose a region 3.5° away. We can produce Uchiyama’s results by choosing a background region similar to Uchiyama’s. For further details, see Aliu et al. [2013].

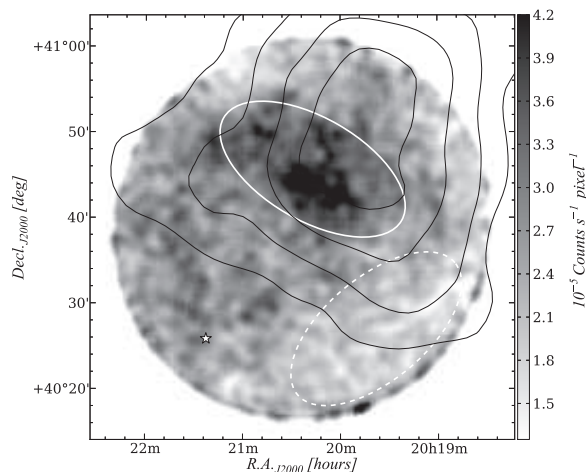


Figure 3: ASCA X-ray view of G78.2+2.1 between 1 and 3 keV, overlaid with the VER J2019+407 smoothed photon excess contours (100, 150, 210 and 260 photons). The region used to extract a spectrum and the corresponding background region to the south of the remnant are indicated by white solid and dashed ellipses, respectively. A white star marks the position of PSR J2021+4026.

5. Interpretation

It is plausible that the VHE γ -ray emission seen from γ -Cygni arises from particles accelerated in shocks occurring at the interaction of the supernova ejecta and the surrounding medium. These particles could be either accelerated electrons, which would produce the emission via inverse-Compton scattering, or accelerated nuclei. Should they be high-energy electrons, they would also be expected to produce X-ray synchrotron radiation, which would appear as a non-thermal power-law component in the X-ray spectrum. While our analysis of the ASCA X-ray spectrum does not argue for a non-thermal component, our upper limit on this component is still weak enough that we cannot exclude the possibility that the TeV, if not the GeV, emission is due to inverse-Compton scattering [Aliu et al. 2013]. On the other hand, it is also plausible that the VHE γ -ray emission is produced by interaction of accelerated nuclei with the H I shell surrounding the remnant. Estimates of the target material density required for accelerated nuclei to produce the observed VHE γ -ray flux, based on Drury et al. [1994], give a range of densities $1.0 - 5.5 \text{ cm}^{-3}$ [Aliu et al. 2013] consistent with Gosachinskij [2001]’s estimates of the gas density within the H I shell. However, it must be noted that the shock velocities inferred from the optical and X-ray data are too low for the forward shock to be currently accelerating particles to TeV energies. If the VHE γ -ray emission is hadronic, it is likely due to particles accelerated when the remnant was younger

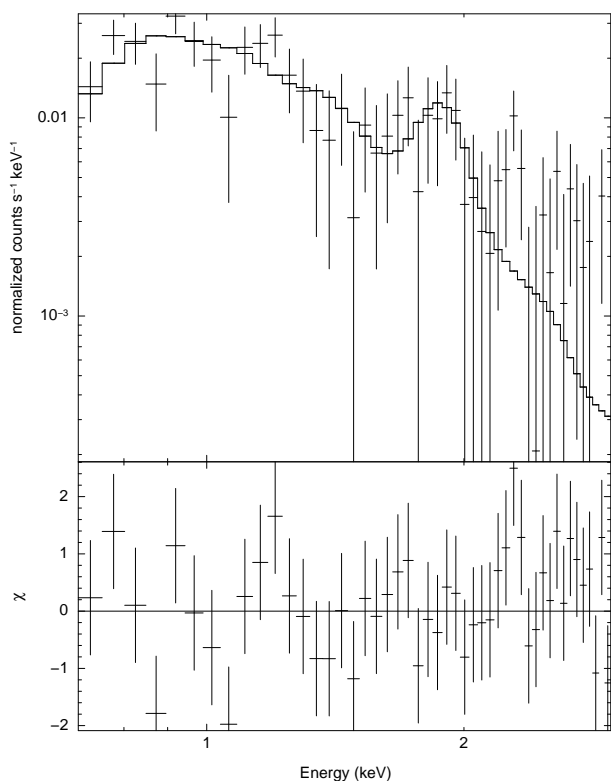


Figure 4: Top Panel — ASCA X-ray spectrum of the region of enhanced X-ray emission coincident with VER J2019+407 shown in Figure 3. The stepped line shows the fit of a Raymond-Smith thermal plasma model with parameters as given in the text. Bottom Panel — residuals from the best-fit model.

that are now interacting with the shell.

The relationship of the cocoon of freshly-accelerated cosmic rays detected by *Fermi* to SNR G78.2+2.1 and VER J2019+407 also remains unclear. It is possible SNR G78.2+2.1 either has injected or is injecting accelerated particles into the cocoon. However, while they are shown for reference, we caution against using the cocoon contours from Ackermann et al. [2011] to judge the relationship of the cocoon to the VHE γ -ray emission, since they are derived from an analysis where 1FGL J2020.0+4049, which is no longer considered an independent source, was included as part of the background model. It should also be noted that the VHE γ -ray excess map in this paper was made with the ring-background estimation method, which is ill-suited to detecting a large-scale (~ 4 square degree) region of γ -ray emission such as the cocoon. Therefore the VHE γ -ray maps shown here cannot be used to set a meaningful upper limit on cocoon emission above 300 GeV. A conclusion determination of the relation-

ship between SNR G78.2+2.1 and VER J2019+407 will have to await further data, analyzed with more sophisticated analysis techniques.

Acknowledgments

This research was supported by grants from the U.S. Department of Energy, the U.S. National Science Foundation and the Smithsonian Institution, by NSERC in Canada, by Science Foundation Ireland and by STFC in the UK. We acknowledge the work of the technical support staff at the Fred Lawrence Whipple Observatory and at the collaborating institutions in the construction and operation of the instrument. Amanda Weinstein and Vikram Dwarkadas acknowledge the support of NASA grant NNX11AO86G. The Cygnus cocoon contours were graciously provided in electronic form by the Fermi LAT team.

References

- Abdo, A. A. et al. 2010, *ApJS*, 188, 405
 Abdo, A. A., et al. 2010, *ApJS*, 187, 460
 Ackermann, M. et al. 2011, *Science*, 334, 1103
 Aliu et al. 2013, submitted.
 Drury, L. O'C., Aharonian, F.A., and Völk, H.J. 1994, *AAP*, 287, 959-971
 Fukui, Y., & Tatematsu, K. 1988, *IAU Colloq.* 101: Supernova Remnants and the Interstellar Medium, 261
 Gosachinskij, I. V. 2001, *Astronomy Letters*, 27, 233
 Higgs, L. A. et al. 1977, *AJ*, 82, 718
 Holder, J., Atkins, R. W., Badran, H. M., et al. 2006, *Astroparticle Physics*, 25, 391
 Ladouceur, Y., & Pineault, S. 2008, *AAP*, 490, 197
 Lande, J., Ackermann, M., Allafort, A., et al. 2012, *ApJ*, 756, 5
 Landecker, T. L., Roger, R. S., & Higgs, L. A. 1980, *AAPS*, 39, 133
 Lozinskaya, T. A. et al. 2000, *Astronomy Letters*, 26, 77
 Mavromatakis, F. 2003, *AAP*, 408, 237
 Nolan, P. L., Abdo, A. A., Ackermann, M., et al. 2012, *ApJS*, 199, 31
 Taylor, et al. 2003, *AJ*, 125, 3145
 Trepl, L., et al. 2010, *MNRAS*, 405, 1339-1348
 Uchiyama, Y. et al. 2002, *ApJ*, 571, 866
 Zhang, X., Zheng, Y., Landecker, T. L., & Higgs, L. A. 1997, *AAP*, 324, 641